

# Journal of Biomedical Optics

BiomedicalOptics.SPIEDigitalLibrary.org

## **Differential *in vivo* urodynamic measurement in a single thin catheter based on two optical fiber pressure sensors**

Sven Poeggel  
Dineshbabu Duraibabu  
Daniele Tosi  
Gabriel Leen  
Elfed Lewis  
Deirdre McGrath  
Ferdinando Fusco  
Simone Sannino  
Laura Lupoli  
Juliet Ippolito  
Vincenzo Mirone

# Differential *in vivo* urodynamic measurement in a single thin catheter based on two optical fiber pressure sensors

Sven Poeggel,<sup>a,\*</sup> Dineshbabu Duraibabu,<sup>a</sup> Daniele Tosi,<sup>a,b</sup> Gabriel Leen,<sup>a</sup> Elfed Lewis,<sup>a</sup> Deirdre McGrath,<sup>c</sup> Ferdinando Fusco,<sup>d</sup> Simone Sannino,<sup>d</sup> Laura Lupoli,<sup>d</sup> Juliet Ippolito,<sup>d</sup> and Vincenzo Mirone<sup>d</sup>

<sup>a</sup>University of Limerick, Department of Electronic and Computer Engineering, Optical Fibre Sensors Research Centre, Main-building C2-051, Limerick 00000, Ireland

<sup>b</sup>Nazarbayev University, School of Engineering, Electrical & Electronic Engineering, 53 Kabanbay Batyr, Astana 010000, Kazakhstan

<sup>c</sup>University of Limerick, Graduate Entry Medical School, Faculty of Education & Health Sciences, Limerick 00000, Ireland

<sup>d</sup>Federico II University of Naples, Scuola di Medicina e Chirurgia, Urologic Clinic, Naples 80121, Italy

**Abstract.** Urodynamic analysis is the predominant method for evaluating dysfunctions in the lower urinary tract. The exam measures the pressure during the filling and voiding process of the bladder and is mainly interested in the contraction of the bladder muscles. The data arising out of these pressure measurements enables the urologist to arrive at a precise diagnosis and prescribe an adequate treatment. A technique based on two optical fiber pressure and temperature sensors with a resolution of better than 0.1 cm H<sub>2</sub>O (~10 Pa), a stability better than 1 cm H<sub>2</sub>O/hour, and a diameter of 0.2 mm in a miniature catheter with a diameter of only 5 Fr (1.67 mm), was used. This technique was tested *in vivo* on four patients with a real-time urodynamic measurement system. The optical system presented showed a very good correlation to two commercially available medical reference sensors. Furthermore, the optical urodynamic system demonstrated a higher dynamic and better sensitivity to detect small obstructions than both pre-existing medical systems currently in use in the urodynamic field. © 2015 Society of Photo-Optical Instrumentation Engineers (SPIE) [DOI: 10.1117/1.JBO.20.3.037005]

Keywords: optical fiber pressure sensors; *in vivo*; urodynamic; pressure; differential; catheter; Fabry–Perot interferometer; fiber Bragg grating.

Paper 140815R received Dec. 9, 2014; accepted for publication Feb. 16, 2015; published online Mar. 10, 2015.

## 1 Introduction

Urodynamic analysis is a key asset for the advanced diagnostics of bladder-related conditions<sup>1,2</sup> and to date the only form of medical test with which to determine the overall functioning of the lower urinary tract (LUT). This includes detection and possible localization of pathological obstruction.<sup>2–4</sup> The urodynamic procedure involves reproducing the functionality of the urinary tract during one or multiple cycles of filling and voiding the bladder. Using a catheter, saline solution is infused in the patient's bladder at a constant rate over a short time. Thereafter, the patient is asked to urinate (i.e., voiding the bladder).

Most of the key information for diagnostics is gathered by recording the functionality of the detrusor muscle when subjected to the bladder filling/voiding process.<sup>2</sup> Detrusor pressure is estimated by measuring the bladder pressure with a catheter, and subtracting the abdominal pressure recorded with a second catheter inserted in the rectum. Currently, most pressure sensors for urology are based on microelectromechanical systems (MEMS) transducers connected to fluid-filled or air-charged catheters. Fiber optic sensors (FOSs) are the main alternatives to MEMS for biomedical applications.<sup>5</sup> Fiber optic-based sensors do not return significant competitive advantages over MEMS, as the early generation of optical fiber pressure sensors (OFPSs) yielded similar performances in terms of accuracy and size with respect to MEMS. More recent developments in

pressure sensors based on extrinsic Fabry–Perot interferometer (EFPI) principle<sup>6,7</sup> enable the manufacture of more compact sensors, with diameters inferior to 0.3 mm and which have a typical accuracy of 2 cm H<sub>2</sub>O. EFPI sensors are based on a Fabry–Perot cavity built on the tip of an optical fiber and sealed with a pressure-sensing diaphragm on the fiber tip. Several solutions for EFPI sensors in biomedical applications have been recently reported.<sup>8–11</sup> Another development is the integration of an EFPI sensor with a temperature sensor based on a fiber Bragg grating (FBG) which allows dual pressure/temperature sensing with mutual compensations of both temperature and pressure as an extension to the state-of-the-art EFPI sensor.<sup>12,13</sup>

Biocompatibility is one of the main barriers for the adoption of EFPI sensors in the urological field. The international organization for standardization (ISO) 10993<sup>14</sup> is the main standard that regulates the insertion of medical devices *in vivo*. All-glass designs are inherently compliant with biocompatibility requirements, whereas most epoxy-based EFPI designs<sup>15</sup> are often not compliant with the ISO standard without appropriate measures being taken. Sufficient mechanical strength of the diaphragm tip is another essential requirement. Although the sensor is protected by the catheter packaging, sub-mm thick<sup>16</sup> or bendable<sup>17</sup> diaphragms may lead to excessive fragility.

The miniature size of fiber-optic EFPI sensors allows multiple probes to be embedded in a single catheter, which is the

\*Address all correspondence to: Sven Poeggel, E-mail: [sven.poeggel@ul.ie](mailto:sven.poeggel@ul.ie)

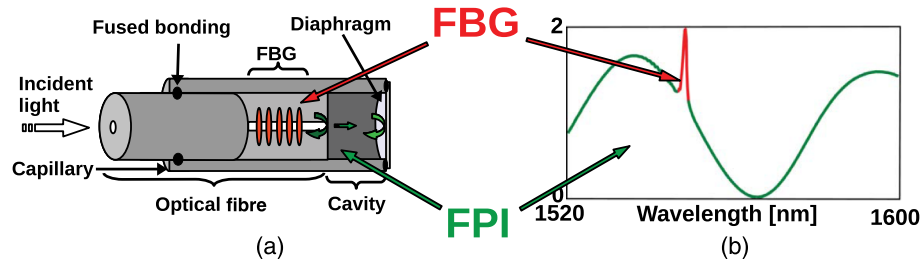


**Fig. 1** (a) The optical fiber pressure and temperature sensor (OFPTS) based on a single-mode fiber (SMF) with internal fiber Bragg Grating (FBG). (b) OFPTS spectrum: illustrating the superposition of the FBG peak and the broadband Fabry–Pérot interferometer (EFPI) spectrum.

same size as a standard urology catheter, e.g., 5–9 Fr (1.6–3 mm), employed in the urodynamic exam. This multiprobe approach allows the measurement of pressure in different locations within the bladder/urethra without creating obstruction. In typical clinical practice,<sup>2</sup> the detection of bladder obstruction through the urodynamic examination involves the measurement of detrusor pressure and flowmetry. This procedure provides the urologist with a qualitative estimator of the patient’s bladder obstruction exhibiting a relatively wide and ambiguous range of urinary flow. Implementing multipoint pressure measurement inside the bladder can progress the currently limited diagnostic method by allowing pressure to be recorded both before and after a potential obstruction. Accuracy, however, is a key requirement. The initial pressure difference between two measurement points is limited to  $\sim 10$  cm H<sub>2</sub>O, and typically less than 5 cm H<sub>2</sub>O.<sup>2</sup> The sensor used in this paper has a 0.1 cm H<sub>2</sub>O ( $\sim 10$  Pa) resolution with  $\pm 0.1$  cm H<sub>2</sub>O accuracy,<sup>13</sup> far better than the recommended pressure accuracy for the existing urodynamic measurements.<sup>2</sup>

Recently, in 2014, we presented the use of EFPI-based sensors in urology,<sup>18</sup> demonstrating that fiber-optic sensors can replace the current pressure transducers. In this work, we present a new catheter structure that is based on a pair of optical fiber sensors. The sensor based on a combination of EFPI and FBG for dual pressure and temperature measurement achieves  $\pm 0.1$  cm H<sub>2</sub>O accuracy. The all-glass design of the sensor is biocompatible with a diameter of 0.2 mm. The sensor is based on bend-insensitive fibers, which allows on-line pressure measurement even when mechanical stress and tight bending are applied. A pair of probes were embedded in a medical catheter of 5 Fr (1.6 mm) thickness, for the measurement of bladder pressure in two active points at 1 cm distance from each other. Experimental online measurements were carried out *in vivo* on four patients. We herein report on the differential pressure measurement recorded during the testing, highlighting the potential use of such metrics for advanced urological diagnostics. The miniature sensor size allows multiple sensors in a single catheter and biocompatibility is the key feature for mapping multiple sensing points in urological diagnostic. To the best of our knowledge, we report the first differential bladder pressure measurement in a single catheter based on fiber optic sensors.

## 2 Overview of the Pressure Sensing Technology

The combined optical fiber pressure and temperature sensor (OFPTS) is based on two separate wavelength modulations, namely an FPI and an FBG, both contained within one single-mode fiber (SMF).

### 2.1 Structure and Fabrication

The pressure and temperature sensor is essentially an optical fiber with an internal FBG and a reflecting diaphragm. The SMF is a low bend loss fiber with draw tower gratings from FBGs<sup>19</sup> with a cladding diameter of 125  $\mu$ m and a mode field diameter of 6  $\mu$ m, and is encapsulated by a glass capillary (inner diameter of 130  $\mu$ m; outer diameter of 200  $\mu$ m). The capillary is fused by a Siecior fusion splicer M90 to the SMF on one side and sealed on the other side with an optical power-core multimode glass fiber (o.d. of 200  $\mu$ m). The power-core fiber is polished with 0.3  $\mu$ m corning-sized diamond polish paper down to  $\sim 6 - 10$   $\mu$ m. Afterward, the diaphragm thickness is reduced by hydrofluoric (HF)-acid to  $h \sim 2$   $\mu$ m.<sup>20</sup> This construction forms a pressure sensitive three-mirror EFPI with a very thin diaphragm, as shown in Fig. 1(a). After the etching process, the pressure sensors exhibit a stability of better than 1 cm H<sub>2</sub>O/hour with a resolution of more than 0.1 cm H<sub>2</sub>O, tested in a 60 cm burette filled with water. The FBG is inscribed in the core of the SMF in close proximity to the point of measurement of the EFPI. The light travels from a broadband light source (BLS) to the end of the fiber-tip [i.e., the end of the sensor, as shown in Fig. 1(a)]. The reflected signal returns to an optical spectrum analyzer (OSA). The light from the FBG is partially reflected before reaching the tip of the fiber. This results in a high intensity of reflection at a particular wavelength, depending only on temperature and strain.<sup>21</sup> The narrow band reflection is shown in Fig. 1(b) by a sharp peak in the 1550 nm wavelength range.

Since the sensor is made of glass only, sensitivity parameters are determined by the Young’s modulus ( $E$ ) and the Poisson’s ratio ( $\mu$ ), as described in Eq. (1). The structure of the sensor allows the end mounted diaphragm to bend (i.e., changing the cavity length  $\Delta G$ ) by

$$\Delta G = \frac{3}{16} \cdot \frac{(1 - \mu^2)}{E} \cdot \frac{r^4}{h^3} \cdot \Delta P, \quad (1)$$

with the presence of externally applied pressure ( $\Delta P$ ). Furthermore, the sensitivity changes dramatically with the thickness of the diaphragm ( $h$ ) and the radius of the sensor ( $r$ ). The internal FBG is used for temperature measurements and for temperature compensation of the EFPI.<sup>22</sup>

### 2.2 Optical Fiber Pressure and Temperature Sensor Placed in a Medical Catheter

The pressure sensor is placed at the end of a 1 m optical fiber. The bend insensitive fiber combined with additional algorithms

supports a bend radius of less than 5 mm. The end of the fiber is spliced to a buffered and jacketed 5 m SMF-28 fiber and terminated using an FC- angle polished connector (FC-APC). The sensors are guided through a Y-junction as shown in Fig. 2(a) up to the tip of the catheter. Two OFPTSs were placed into a 5 Fr nutrisafe 2 catheter (REF 361.052) from Vygon with a length of 50 cm. The fiber is externally glued to the outside of the Y-junction to guarantee a stable placement (with no interference of glue and saline solution) of the tip of the sensor between hole one and two and behind hole two and three in a 1 cm distance. The glue also seals the end of the catheter completely, which is mandatory for an accurate measurement.

The Y-junction also allows the infusion of 0.9% saline solution to remove air from the catheter. This prevents a rapid change of the refractive index from saline solution ( $n \sim 1.34$ ) to air ( $n \sim 1$ ). The whole catheter-sensor structure can be easily replaced by connecting two new sensors to the FC-APC of the system. Figure 2(b) photographically shows the catheter with sensors used during the urodynamic measurement.

### 2.3 Optical Urodynamic System

The optical urodynamic system (OUS) is shown in Fig. 3(a). The BLS (EXS210069-01) from Exalos has a Gaussian shape output with a power of 14.97 mW and a bandwidth of 46.2 nm at 1554.2 nm. The amplified spontaneous emission ripple is quoted as 0.074 dB over a wavelength range of 0.5 nm. The source is connected to a 3-dB splitter guiding the light to an optical switch from Sercalo (SW1x4-9N) with a 1 ms switching time and a 1.0 dB insertion loss, based on micromechanical mirrors. The light is reflected (at the FBG and EFPI) and guided back to the OSA (IMON-512 from Ibsen Photonics with a bandwidth from 1510 to 1596 nm). The OSA has a resolution of 512 pixels corresponding to a peak shift of the EFPI spectrum of 0.166 nm. The relatively low spectral resolution is compensated by algorithms developed for EFPI pressure measurements, which also compensate for any signal artifacts and rapid changes of saline concentration. The optical switch was operated with a frequency of 20 Hz in an interval of 5 frames/cycle and 2 cycles/sensor resulting in a 10 Hz sample rate for each sensor, as recommended for urodynamic analysis.<sup>2</sup> An Arduino one board triggered the optical switch and activated the OSA with a time delay of 2 ms to allow the optical switch to stabilize. The signal was acquired for 20  $\mu$ s, however, this could be varied depending on the reflectivity of the sensor (i.e., weaker gratings and higher loss in splicing need a higher acquisition time). The complete system is housed in a hand case for protection and ease of transport.

The software is based on a three-layer concept. First, the synchronization of the switch and optical spectrum analyzer was timed by an Arduino one board programmed in C. The OSA acquired the light from the sensor and buffered the frames internally in an internal buffer. Second, a server programmed in C++ communicates to the interrogator and provides the frames (i.e., measurement of the intensity of the reflected spectrum) as packages to a client over a network protocol. Finally, the client was an in-house developed LabView program designed for urodynamic analyses. The graphical user interface is shown in Fig. 3(b) and shows three main graphs, indicating the pressure trace of both OFPTSs and a third graph for differential pressure. The software also compensates for small bending and changes in the refractive index of the saline medium. An internal additional algorithm was developed to overcome the relatively low spectral resolution of the interrogator and to achieve a high resolution of better than 0.1 cm H<sub>2</sub>O.<sup>13</sup>

## 3 Measurement Setup

Urodynamic analysis is a two-fold study of the filling cystometry and the pressure-flow study of the LUT, which includes the bladder and urethra. The bladder is surrounded by the detrusor muscle which contracts during urination. A normal/healthy bladder may contain 300 to 500 ml of fluid and the urination process can reach a flow rate of >15 ml/sec.<sup>23</sup> The real-time *in vivo* urodynamic analysis presented in this paper was achieved using simultaneous measurement by the optical and standard medical equipment. Different sensors and devices were used to provide a range of measurements.

### 3.1 Setup of the Equipment

In Fig. 4, the OUS is shown on the left-hand side, whereas the medical equipment is schematically shown on the right-hand side. In each patient, two commercially available medical sensors were placed in the bladder and in the rectum, respectively. A separate catheter was placed in the bladder to facilitate the filling phase with saline solution and a dynamic flowmeter was used to analyze the flow rate of urine during voiding.

### 3.2 Medical Reference Sensor: PICO-2000 and SmartDyn

To guarantee an appropriate measurement comparable with current gold standard urodynamic systems [Figs. 5(a) and 5(b)], two commercial systems were used and the results were compared with the OUS under identical conditions. The PICO-2000 is a urodynamic system produced by MenFis bioMedica.<sup>24</sup> The second system provided by Albyn Medical Ltd. is called

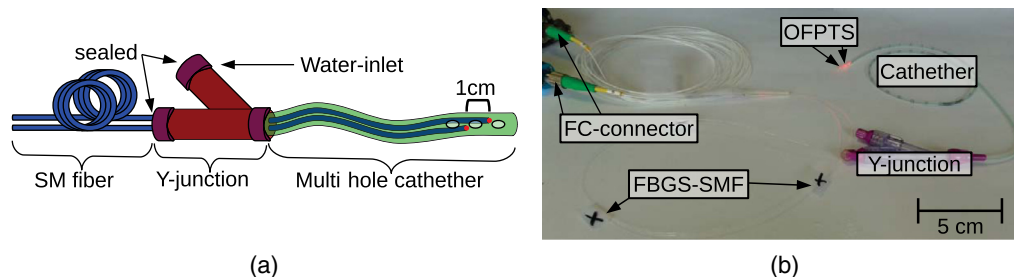


**Fig. 2** (a) The schematic diagram of the OFPTS in a medical catheter. Both sensors are placed at a 1 cm distance to each other and sealed by a Y-junction. (b) The photograph of both sensors illuminated by a red light to identify the position in the catheter.

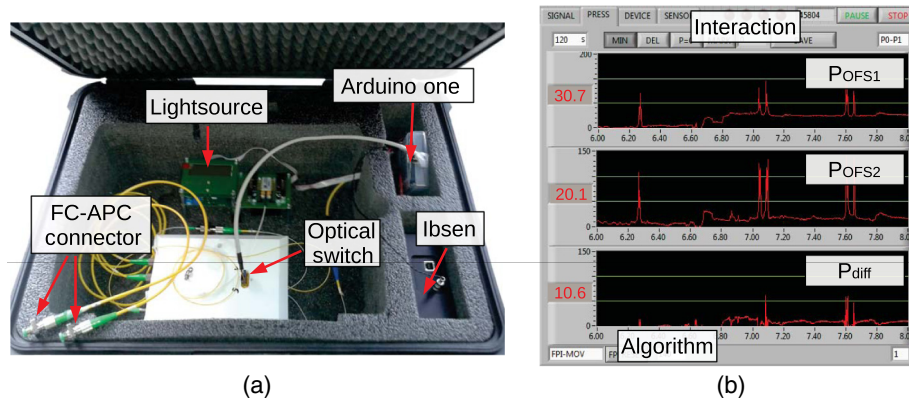


**Fig. 3** (a) The optical urodynamic system (OUS), based on a light source, 3-dB coupler, Arduino one board, an optical switch (4 ports) and an optical spectrum analyzer (OSA). Everything fits in a hand case for easy transport and protection. (b) The graphical user interface (GUI) of the urinary measurement. The first graph shows the pressure trace of the first OFS in the tip ( $P_{OFS_1}$ ). The second graph shows the pressure of the second OFS ( $P_{OFS_2}$ ) and the third graph shows the differential pressure ( $P_{diff}$ ) between the first and second sensors.

SmartDyn. Both systems are based on electronic sensors, measuring a differential pressure in the bladder (i.e., the intravesical pressure  $P_{ves}$ ) and the abdomen (i.e., the intra-abdominal pressure  $P_{abd}$ ). The SmartDyn system is available with a main control which connects the sensor, flowmeter, and infusion system. The flowmeter is based on a gravimetric measurement whereby the patient urinates into a beaker placed under a chair. This is used to analyze the speed and volume during urination (dynamic flow analysis). Additionally, a controlling system infuses saline solution through the urethra into the bladder of the patient. All measurements are collected and transferred to a PC. Figure 5(a) shows the desk with the laptops and the OUS in the background. The first laptop was used to analyze the OFPTS, the second laptop was wirelessly connected to the SmartDyn system.

### 3.3 Examination and Preparation

To analyze lower urinary tract symptoms (LUTSs) (e.g., incontinence, urgency to urinate),<sup>23</sup> the patient needs to undergo a cystometrogram (CMG) which involves filling the bladder with saline solution (~0.9% salt concentration). In a healthy bladder, the result is a minimal increase in pressure, however, if the bladder pressure increases beyond a determined point, this indicates that the bladder is unhealthy and lacks elasticity (known as bladder compliance).<sup>25</sup> The pressure-volume relation depends on various factors, e.g., gender, shape, and volume of the bladder.<sup>26</sup> Furthermore, dynamic pressure responses caused by coughing or

talking may simultaneously affect the bladder and abdomen. When the patient starts to urinate the detrusor muscle applies pressure mainly on the bladder. This can be expressed in

$$P_{det} = P_E - P_{abd}, \tag{2}$$

where  $P_{det}$  is the pressure of the detrusor (i.e., the differential pressure),  $P_{ves}$  is the pressure measured in the bladder, and  $P_{abd}$  is the measured pressure in the rectum.<sup>2</sup>

The complete process of filling the bladder through voiding is generally measured *in vivo* using pressure probes in both the bladder and rectum. A pressure-flow study measures the pressure of the bladder with additional analysis of the flow rate as measured by a flowmeter.<sup>23</sup> The pressure measurement is recorded by two sensors, one placed in the bladder and the other in the rectum. In the work presented here, an alternate method is investigated, whereby two sensors have been inserted in the same urethra catheter at a distance of 1 cm apart. The first sensor is placed in the bladder ( $OFS_1$ ) and the second close to the urethra ( $OFS_2$ ). The distance of 1 cm was chosen based on the functional profile length over the maximum urethral pressure.<sup>27</sup> The highest pressure change ( $\Delta P$ ) can be observed over a 1 cm distance, which can be used as an indicator for correct placement. During the insertion process, when both sensors show a similar pressure measurement (i.e.,  $P_{diff}$  is comparatively small), both sensors are correctly placed. The differential pressure ( $P_{diff}$ ) is calculated by

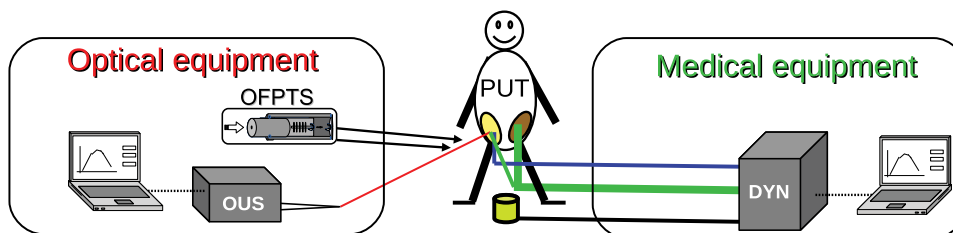


**Fig. 4** The figure shows the schematic of the optical and standard medical equipment. From the optical urodynamic system, one catheter with two sensors was inserted. The medical equipment (DYN) consists of two separate catheters for each sensor (middle catheter) and an additional catheter (on the top) to fill the bladder with saline solution. During the urination process, a flowmeter was used to analyze the urinary flow rate.

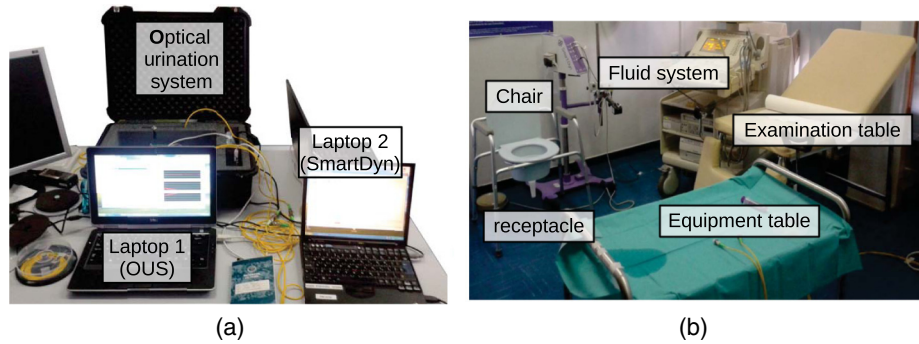


**Fig. 5** (a) The measurement of the urination process is simultaneously analyzed on each laptop. (b) The examination room is separated by a curtain in two areas. The main area contains the examination table where the patient is placed during the insertion of the sensor.

$$P_{diff} = P_{OFS_1} - P_{OFS_2} \quad (3)$$

Before the examination starts, the patient is placed on the examination table [Fig. 5(b)] and both commercial sensors in the catheters are guided through (1) the urethra into the bladder and (2) into the rectum of the patient. The catheter with both OFPTSs is inserted afterward, as shown schematically in Fig. 6. The entire length of the catheter was inserted deep inside the bladder to ensure that both OFPTSs were placed well inside the lumen (cavity). In this way, both sensors were able to record the same pressure, regardless of the variable patient anatomy. After this, the patient was made to cough and if both optical sensors were approximately sensitive to the cough, it was considered that the sensors were fully inside the urethra.

The urodynamic examination is divided into two phases. In the first phase, the patient is asked to cough several times to test all sensors and the bladder is infused with saline solution (CMG). At the end of this phase, the bladder reaches a certain maximum of volume capacity at which point the patient starts to feel the urge to empty the bladder which indicates that the bladder is fully contracted. The patient then moves to the urination chair for the voiding phase (pressure flow study). Since the sensors are moving and bending during this time, the equipment may have to be moved or even disconnected rendering the pressure readings irrelevant. In the second phase, the patient empties the bladder into a receptacle with a flowmeter situated below recording the volume of urine. In a healthy patient, the muscles contract and squeeze the urine out of the bladder during

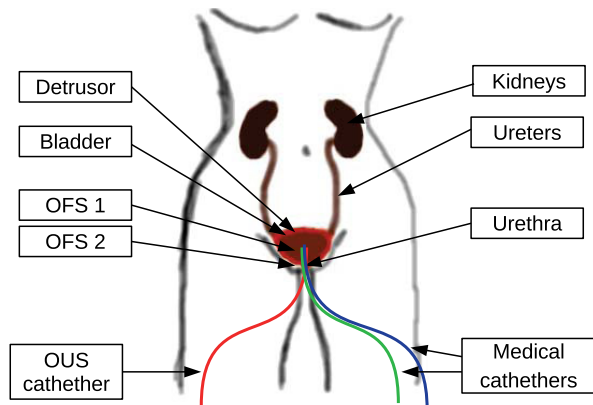


**Fig. 6** Anatomy of female patient.

urination. In a patient who exhibits a urological disorder this function may be impaired or may not work at all.

## 4 Urodynamic Experimental Results

A number of results arising from the urodynamic measurement cycles of four patients with urological disorders were recorded over a period of several days at the urology clinic of the Federico II University Hospital in Naples, Italy. Catheter type and medical equipment were altered to guarantee a variety of devices and to investigate the OFPTS under different conditions.

### 4.1 Feasibility Test with Bend-Sensitive Fiber-Based Sensor

To investigate the feasibility of an optical fiber sensor in a urodynamic measurement, a single OFPTS was tested *in vivo* in the bladder of a female patient. The commercial medical sensor, used as reference sensor in this measurement, was the PICO-2000. In the first part, the bladder is infused with saline solution, which results in an increase of the bladder pressure ( $P_{ves}$ ). Both sensors show a very good correlation during the infusion, with a correlation factor of  $R^2 = 0.93$ , as shown in Fig. 7. As soon the bladder contraction starts, the patient is moving from the examination bed to the urodynamic chair, causing a high bend in the bend sensitive fiber. The pressure trace is still observable but the correlation factor of both sensors is reduced to  $R^2 = 0.01$ . In the last phase, the patient is in the voiding phase. The bladder contractions are measured by both sensors with a high correlation of  $R^2 = 0.81$ .

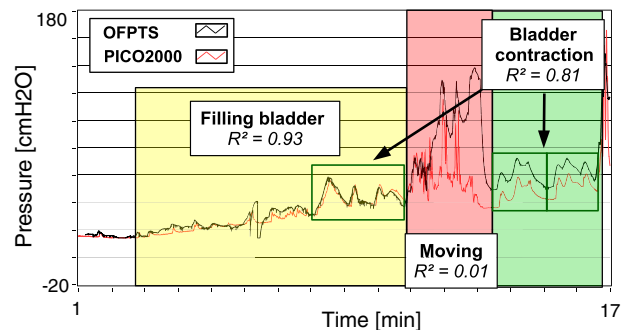


**Fig. 7** The comparison of the PICO-2000 and the OFPTS shows a good correlation. During the movement of the patient, the bend sensitive fiber lost the signal, causing an offset in the measurement.

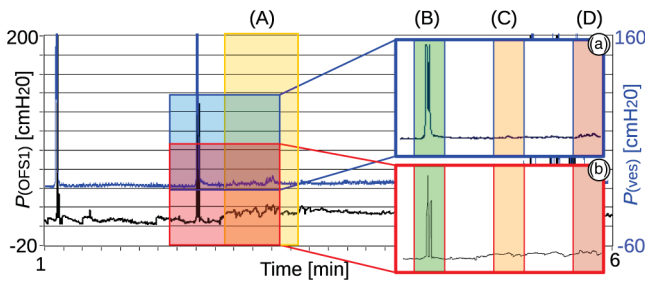


**Fig. 8** A 5-min measurement of the patient with infusion of saline solution in (A) results in a variation of pressure. (a) A 1-min measurement during cough and infusion of the SmartDyn system. (b) The same time period as (a) with the OFPTS.

Since the fiber is highly sensitive to bending which can cause a variation in the reflected signal, the online interpretation of the data during the 16 min *in vivo* analyses was inaccurate. However, in postanalysis, the high degree of correlation of both sensors became evident.

### 4.2 High Sensitivity with Bend-Insensitive Sensor

The sensors were initially built by a corning optical fiber (SMF-28). Further investigation demonstrated that the bending during the examination changed their reflected spectrum with a bend radius below ~2 cm, causing artifacts which affect the online measurement. As a result, the SMF of the OFPTS was replaced with bend insensitive fibers from FBGS. Furthermore, the PICO-2000 system was changed to a more advanced medical urination system (i.e., SmartDyn). Figure 8 shows the recorded pressure data from an online measurement, comparing the OFPTS with the SmartDyn sensor.

The patient's cough in instances (B) have both similar values, indicating a good correlation. The period covered by part (A) shows when the bladder was being filled with 200 ml of saline solution. The volume of the infusion is controlled and recorded by the SmartDyn system. The SmartDyn sensor shows a pressure increase of ~10 cmH<sub>2</sub>O, whereas the OFPTS increase

~20 cmH<sub>2</sub>O. Even with an initialized time resolution corresponding to a sampling frequency of 10 Hz, the details of the OFPTS are clearer than those of the medical sensor. The peak in (B) measured by the OFPTS in Fig. 8(b) shows two peaks per cough. The SmartDyn sensor in Fig. 8(a) shows an envelope of both peaks. This explains the smooth signal of the SmartDyn sensor during the measurement. The measurement of the OFPTS is shown without additional filtering of the pressure measurement, resulting in a more detailed observation.

### 4.3 Dual Optical Fiber Pressure and Temperature Sensors System and the Medical Sensor

The previous analysis demonstrated a good correlation between OFPTS and the commercially available sensors. The high sensitivity of the sensor was capable of detecting even small variations during the saline infusion. Investigation into the reliability of the OUS has to be proved by a simultaneous measurement of all four sensors during a full investigation. An additional examination with both optical sensors (OFS<sub>1</sub> and OFS<sub>2</sub>) in a 5 Fr catheter was used in a full analysis alongside the bladder (ves) and abdominal (abd) sensors. The results from filling the bladder up to the voiding phase are shown in the 14 min measurement in Fig. 9.

In urodynamics, the morphology of the contraction caused by the bladder muscles is important and requires a high precision measurement. Significantly, part (B) shows contraction during the infusion of saline solution with the same pattern in all four sensors. However, only the two OFPTSs show a significant increase in pressure during the infusion time, such as would be the case for a normal healthy bladder.<sup>25</sup> Parts (C) and (D) show a series of coughs and (F) shows the patient's movement, which are not relevant for this urodynamic analysis. (E) shows some contraction of the muscles of the bladder, indicating the urgent need to urinate. The pressure measurement demonstrates that all four sensors are measuring similar pressures, indicating a good correlation.

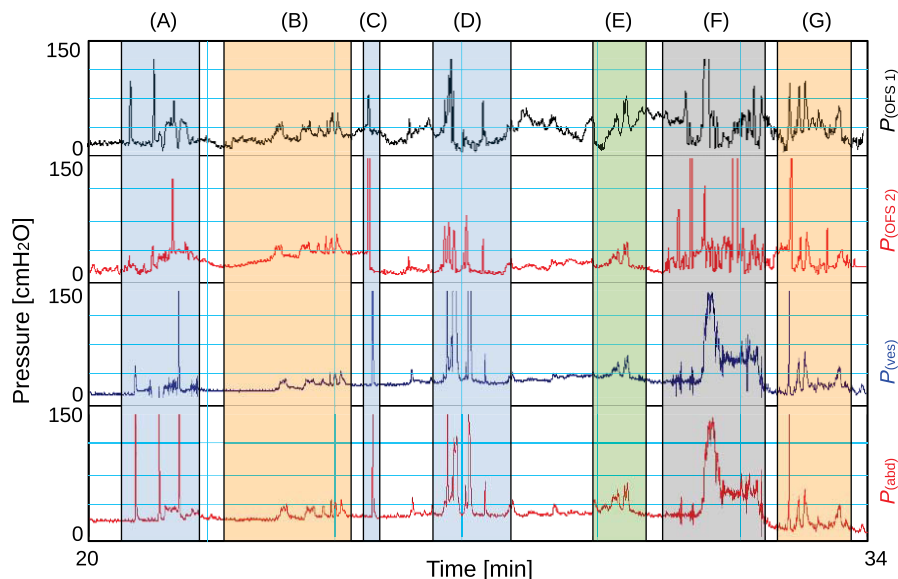


**Fig. 9** Pressure data captured using both OFPTS (i.e., the first in front of the catheter and the second 1 cm behind the first) and the SmartDyn sensors in the bladder and abdomen.

## 5 Medical Interpretation

The experimental results demonstrate the high pressure and time resolution of the optical sensors. The high correlation to the standard medical equipment is a proof of concept. The patients in this study were in overall healthy condition, resulting in a stable body temperature during the measurement. To investigate the new differential method, a full investigation with a male patient was undertaken.

### 5.1 Complete Differential Pressure Analysis

Urodynamic studies are mainly interested in the contraction of the bladder which is generated by the bladder muscles. Other bodily movements such as coughing and talking can affect the pressures generated in the bladder, abdomen, and rectum. To remove this artifact, the differential pressure analysis is calculated [see Eqs. (2) and (3)]. Figure 10(a) shows the pressure measurement of both optical sensors ( $P_{\text{OFS}_1}$  and  $P_{\text{OFS}_2}$ ). The bladder pressure ( $P_{\text{ves}}$ ) and abdominal pressure ( $P_{\text{abd}}$ ) are recorded in Fig. 10(b). Figure 10(c) shows the differential pressure measurement of both techniques. The infusion of saline solution and the voiding volume measured by the flowmeter are shown in Fig. 10(d). The cystometric capacity (CC) indicates a full bladder which results in a higher activity in the pressure change.<sup>2</sup>

During the time of 1 to 11 min, the bladder is filled with saline solution which results in an increase of the volume, as shown by  $V_{\text{inf}}$  in Fig. 10(d). Only the first OFPTS ( $P_{\text{OFS}_1}$ ) is measuring a rise in pressure. In this case, the commercial abdominal sensor measured a pressure increase, resulting in a negative differential pressure, when it was anticipated that the differential pressure would be positive due to the increase in volume. On the other hand, the differential measurement of the

OUS shows an increase in pressure. This can be explained by the high sensitivity of the optical sensors. In our investigation,  $\text{OFS}_1$  was fully inside in the bladder, whereas the second sensor ( $\text{OFS}_2$ ) was close to the patient's urethra. This resulted in the same pressure reading when muscle contraction occurred. The first sensor also measured the increase in pressure caused by the increase of volume in the bladder during infusion. Indeed, all four sensors show the same trend, but only the first optical sensor ( $\text{OFS}_1$ ) shows an increase in pressure with the infusion of saline solution and stays constant after the infusion has stopped.

In the second part (B) of the measurement, the patient started to urinate. The increase in  $V_{\text{uri}}$  in Fig. 10(d) indicates the volume decrease in the bladder as recorded by the flowmeter. During the urination phase, the correlation of both sensors is evident. Furthermore, the differential pressure analysis demonstrates that the small variations are caused by the obstruction since they occur on both optical sensors simultaneously and are completely removed.

### 5.2 Pressure Performance During Infusion and Voiding

A detailed analysis is shown in Fig. 11 which shows the bladder contraction of the patient ( $\text{PAT}_1$ ) directly after the CC from the measurement in Fig. 10. Both sensors ( $\text{OFS}_1$  and  $\text{OFS}_2$ ) show a good similarity, which demonstrates the high sensitivity of the sensors. To compare the structure of the obstruction, a second patient ( $\text{PAT}_2$ ) with a clear contraction trend is also shown on the normalized time graph. Unlike the first patient where small variations in the graph were visible, in the case of  $\text{PAT}_2$  a normal graph was demonstrated. This could be an indicator that  $\text{PAT}_1$  has a urological condition.<sup>2</sup>

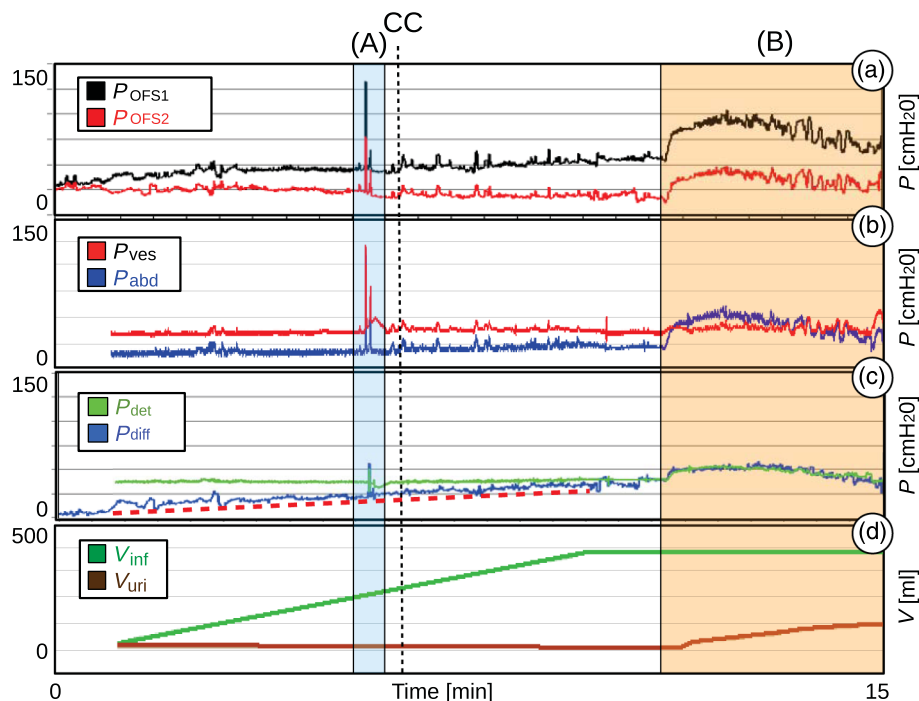


**Fig. 10** (a) The pressure measurement by both OFPTSs. (b) The pressure by the commercial medical reference sensor. (c) Compares the differential pressure of the OUS and the SmartDyn system. (d) The volume of the infusion of saline solution and the volume measured by the flowmeter during voiding the bladder. The cystometric capacity (CC) is reached at 250 ml after the cough, resulting in a higher activity in the pressure change.

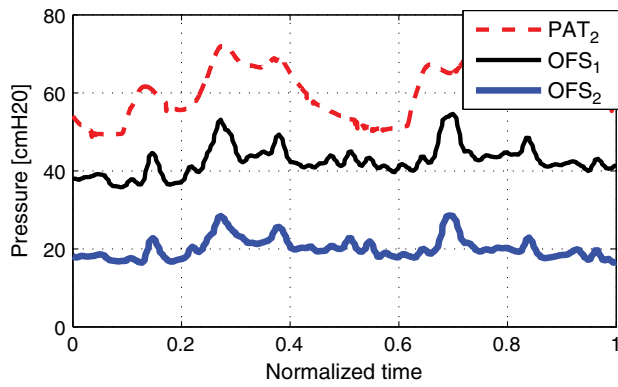


**Fig. 11** Bladder contraction of patient 1 (OFS<sub>1</sub> and OFS<sub>2</sub>), with changed pressure offset (to compare both charts). The bladder contraction of a second patient (PAT<sub>2</sub>) is shown on the normalized time graph to compare the obstruction pattern.

The infusion of saline solution (i.e., increasing of bladder volume) is controlled by the SmartDyn system. This results in an increase in the bladder pressure ( $P_{OFS_1}$ ) only. However, the voiding of the bladder has to be controlled by the detrusor muscle, which affects both sensors. The differential pressure ( $P_{diff}$ ) as a function of the bladder pressure ( $P_{OFS_1}$ ) is shown in Fig. 12(a). The figure is divided into an infusion and a urination (voiding) phase. It is clearly evident that during infusion, only the pressure of the optical sensor in the bladder ( $P_{OFS_1}$ ) has increased. During the voiding (emptying) phase, the slope is smaller ( $m = 0.43$ ) since the differential pressure ( $P_{diff}$ ) during the change of bladder pressure ( $P_{OFS_1}$ ) has become smaller. This can be explained by the fact that the detrusor muscle is affecting the bladder and the urethra (i.e.,  $P_{OFS_1}$  and  $P_{OFS_2}$ ), resulting in a reduced differential pressure.

The function of the differential pressure in relation to the volume after the CC was reached is shown in Fig. 12(b). This demonstrates that the differential pressure is linearly increasing during the infusion with 0.1 cmH<sub>2</sub>O/ml. The same behavior was also demonstrated by Malbrain and Deeren,<sup>28</sup> whereas the voiding phase shows a bigger change in differential pressure ( $P_{diff}$ ) with the change of bladder volume ( $V_{Bladder}$ ). In the

research by Malbrain and Deeren, the infusion is on the right-hand side and the voiding phase is on the left-hand side (i.e., the opposite of this measurement). This could be an indication of a medical condition.<sup>28</sup>

## 6 Conclusion

In our investigation, we demonstrated the use of OFPTSs based on FBG and FPI in urodynamic measurements. Two pressure sensors of 200  $\mu\text{m}$  in diameter, with a resolution of 0.1 cmH<sub>2</sub>O ( $\sim 10$  Pa) and a drift of better than 1 cm H<sub>2</sub>O/hour, were placed into a thin multihole urinary catheter of 5 FR (1.6 mm) in diameter. This allowed the simultaneous measurement of two pressures in different areas of the patient's bladder, therefore, improving the effectiveness of the urodynamic exam and minimizing patient discomfort. In order to analyze the flexibility and accuracy of the sensors in a number of *in vivo* examinations, four patients with a variety of lower urinary tract conditions and two different commercially available urodynamic systems were chosen.

The OFPTS results presented in this paper showed a very high correlation to the gold standard of commercially available sensors, especially during obstruction in an infusion and urination phase. Furthermore, it showed that the optical sensors have better resolution and sensitivity for bladder obstruction than current measurement methods. In a clinical setting, this increased sensitivity has the potential to benefit early patient diagnosis and prompt management. Additionally, the optical pressure sensor showed an increase in pressure in the patient's bladder during the infusion of saline water, whereas the commercially available sensors were not capable of measuring a qualitative change. This demonstrated the sensitivity, accuracy, and effectiveness of the OUS compared to the commercial medical urodynamic system.

In addition, an alternative technique to the existing methods of differential pressure analysis was tested. This state-of-the-art technique used a pressure sensor in both the bladder and the rectum and used the recorded pressure in both points to determine the overall differential pressure. The investigation presented in this paper is using two sensors partially separated in only one small size catheter placed only in the bladder. This urodynamic differential pressure analysis in one multihole

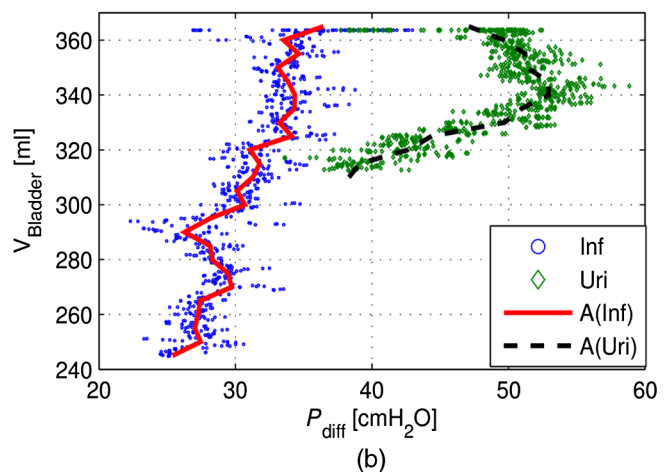
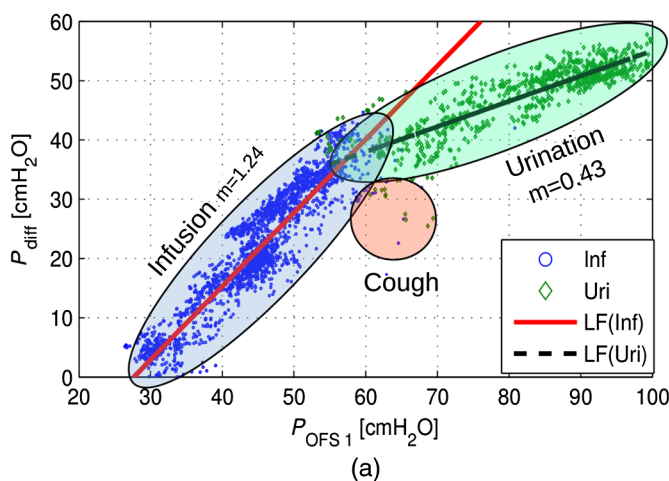


**Fig. 12** (a) Pressure relation of differential pressure  $P_{diff}$  in relation to the bladder pressure  $P_{OFS_1}$  during infusion and urination phase. The slope ( $m$ ) of the linear fit (LF) is plotted for both phases. (b) The volume of the bladder ( $V_{Bladder}$ ) as a function of the differential pressure ( $P_{diff}$ ). The infusion is shown on the left-hand side and the urination on the right-hand side.

catheter was, to the best of our knowledge, the first measurement based on optical fibers.

### Acknowledgments

The authors would like to thank the Chemistry Department, University of Limerick, for use of their facilities. We also would like to thank FBGS for their fibers and Vygon for their Y-junction for our catheters. This work was supported by Science Foundation Ireland (10/RFP/ECE2898), the Marie Curie action (MC-IEF-299985), and the Irish Research Council (EPSPG/2011/343).

### References

- V. W. Nitti, "Pressure flow urodynamic studies: the gold standard for diagnosing bladder outlet obstruction," *Rev. Urol.* **7**(Suppl. 6), S14 (2005).
- W. Schäfer et al., "Good urodynamic practices: uroflowmetry, filling cystometry, and pressure-flow studies," *Neurourol. Urodyn.* **21**(3), 261–274 (2002).
- G. A. Defreitas et al., "Refining diagnosis of anatomic female bladder outlet obstruction: comparison of pressure-flow study parameters in clinically obstructed women with those of normal controls," *Urology* **64**(4), 675–679 (2004).
- A. Kuhn et al., "Sonographic transvaginal bladder wall thickness: does the measurement discriminate between urodynamic diagnoses?," *Neurourol. Urodyn.* **30**(3), 325–328 (2011).
- G. Cote, R. Lec, and M. Pishko, "Emerging biomedical sensing technologies and their applications," *IEEE Sens. J.* **3**, 251–266 (2003).
- P. Roriz et al., "Review of fiber-optic pressure sensors for biomedical and biomechanical applications," *J. Biomed. Opt.* **18**(5), 050903 (2013).
- Y.-J. Rao, "Recent progress in fiber-optic extrinsic Fabry–Perot interferometric sensors," *Opt. Fiber Technol.* **12**(3), 227–237 (2006).
- K. Chin et al., "Fabry–Perot diaphragm fiber-optic sensor," *Appl. Opt.* **46**(31), 7614–7619 (2007).
- P. Polygerinos et al., "MRI-compatible fiber-optic force sensors for catheterization procedures," *IEEE Sens. J.* **10**, 1598–1608 (2010).
- M.-D. Zhou et al., "An implantable Fabry–Perot pressure sensor fabricated on left ventricular assist device for heart failure," *Biomed. Microdevices* **14**(1), 235–245 (2012).
- F. Xu et al., "High-sensitivity Fabry–Perot interferometric pressure sensor based on a nanothick silver diaphragm," *Opt. Lett.* **37**, 133–135 (2012).
- K. Bremer et al., "Conception and preliminary evaluation of an optical fiber sensor for simultaneous measurement of pressure and temperature," *J. Phys.: Conf. Series* **178**(1), 012016 (2009).
- S. Poeggel et al., "Low drift and high resolution miniature optical fiber combined pressure- and temperature sensor for cardio-vascular and other medical applications," in *Proc. 2013 IEEE Sensors*, pp. 1–4 (2013).
- FDA, *Use of International Standard ISO 10993, Biological Evaluation of Medical Devices Part 1: Evaluation and Testing*. U.S. Department of Health and Human Services, draft guidance ed. (2013).
- H. Bae and M. Yu, "Miniature Fabry–Perot pressure sensor created by using UV-molding process with an optical fiber based mold," *Opt. Express* **20**, 14573–14583 (2012).
- C. Liao et al., "Sub-micron silica diaphragm-based fiber-tip Fabry–Perot interferometer for pressure measurement," *Opt. Lett.* **39**, 2827–2830 (2014).
- L. Chen et al., "High performance chitosan diaphragm-based fiber-optic acoustic sensor," *Sens. Actuat. A: Phys.* **163**(1), 42–47 (2010).
- S. Poeggel et al., "Fiber-optic EFPI pressure sensors for *in vivo* urodynamic analysis," *IEEE Sens. J.* **14**, 2335–2340 (2014).
- FBGS, "FBGs—draw tower gratings," Technical Report, FBGS International NV February 2015 V5, <http://www.fbgs.com/contactform/be-en/1/detail/item/3/> (2014).
- S. Poeggel et al., "Novel diaphragm microfabrication techniques for high-sensitivity biomedical fiber optic Fabry–Perot interferometric sensors," *Proc. SPIE* **9098**, 909813 (2014).
- A. Othonos and K. Kalli, *Fiber Bragg Gratings: Fundamentals and Applications in Telecommunications and Sensing*, Artech House, Boston (1999).
- K. Bremer et al., "Feedback stabilized interrogation technique for EFPI/FBG hybrid fiber-optic pressure and temperature sensors," *IEEE Sens. J.* **12**(1), 133–138 (2012).
- C. Dawson, H. N. Whitfield, and P. Cheatham, *ABC of Urology*, 2nd ed., pp. 1–3, Blackwell Publishing Ltd. (2009).
- Menfis bioMedica, <http://www.menfis.it/index2.php?lang=ENG>.
- C. J. Fowler, "Investigation of the neurogenic bladder," *J. Neurol. Neurosurg. Psych.* **60**(1), 6 (1996).
- M. S. Damaser and S. L. Lehman, "The effect of urinary bladder shape on its mechanics during filling," *J. Biomech.* **28**(6), 725–732 (1995).
- P. Abrams et al., "Standardisation of terminology of lower urinary tract function," *Neurourol. Urodyn.* **7**(5), 403–427 (1988).
- M. L. Malbrain and D. H. Deeren, "Effect of bladder volume on measured intravesical pressure: a prospective cohort study," *Crit. Care* **10**(4), R98 (2006).

**Sven Poeggel** is a doctoral student at the University of Limerick, Ireland. He received his BSc and MSc degrees in information technology and technical informatics at the University of Rostock, Germany. His research interests include optical fiber sensors, medical applications, and fluid dynamics. He is a student member of SPIE.

**Dineshbabu Duraibabu** is a PhD student working for the Optical Fiber Sensors Research Centre (OFSRC) at the University of Limerick, Ireland. He received his BE degree in electronics and communication engineering from Anna University, India. His research interests include optical fiber pressure and temperature sensors for marine-based applications.

**Daniele Tosi** is an assistant professor at Nazarbayev University, Astana, Kazakhstan; previously he held a Marie Curie Intra-European fellowship at the University of Limerick, Ireland (2012 to 2014). He received his BEng, MEng degrees in telecommunication engineering, and his PhD degree in electronic engineering from Politecnico di Torino in 2004, 2006, and 2010, respectively. His research interests include fiber-optic pressure sensors, fiber Bragg gratings, and signal processing.

**Gabriel Leen** is a senior research fellow in the Optical Fibre Sensor Research Centre at the University of Limerick. He received his BEng., MEng, and PhD degrees in fields of electronic and computer engineering from the University of Limerick, Ireland, in 1995, 2000, and 2002. His current research interests include optical sensors, fluidics, and medical devices.

**Elfed Lewis** is an associate professor and director of the Optical Fibre Sensors Research Centre, which he founded in 1996. He has authored and coauthored more than 70 journal papers and made in excess of 200 contributions to international conferences. The Optical Fibre Sensors Research Centre under his leadership is engaged in investigating sensors for environmental monitoring, food quality assessment, and parameters of high-power microwave sources and medical devices.

**Deirdre McGrath** is the director of education at the Graduate Entry Medical School and consultant in respiratory medicine in Barringtons Hospital in Limerick. Her key research interests include immunity and inflammation, the clinical application of medical devices, and medical education. She is one of the founding principal investigators of 4i, the centre for interventions in infection, inflammation and immunity, and also she is the medical adviser to the Optical Fibres Sensor Research Centre at the University of Limerick.

**Ferdinando Fusco** is an assistant professor of urology at the University of Naples School of Medicine and Surgery in Naples, Italy. His research interests include lower urinary tract symptoms, urodynamics, sexual dysfunction, and male infertility. He is actively involved in several preclinical and clinical scientific research protocols in these specialty areas, and routinely manages out-patient clinics dedicated to male and female LUTS, neurourology, and male sexual and reproductive dysfunctions.

Biographies of the other authors are not available.